Int. J. Heat Mass Transfer. Vol. 35, No. 1, pp. 165–173, 1992
Printed in Great Britain

0017-9310/92 $5.00+0.00

Some characteristics of the inclined, closed tube thermosyphon under low Rayleigh number conditions

G. S. H. LOCK and J. D. KIRCHNER
Department of Mechanical Engineering, University of Alberta, Edmonton, Alberta, Canada T6G 2G8

(*Received* 20 *March* 1990 *and in final form* 3 *January* 1991)

Abstract—An experimental investigation of single-phase heat transfer in the closed tube thermosyphon inclined at various angles to the vertical is reported. With water as the filling fluid, the system is studied over a range of low Rayleigh numbers extending almost two orders of magnitude. Heat transfer data for a tube with equal heated and cooled lengths are presented and discussed along with a conceptual model of the internal flow.

INTRODUCTION

THE TUBULAR single-phase thermosyphon has received much attention in recent years [1–9]. In closed form it has many applications, ranging from the cooling of gas turbine blades to the improvement of waste heat exchangers. Perhaps its most widespread use is in a northern geotechnical context where it provides a means whereby the virtually infinite source of cold winter air may be employed to create and maintain frozen ground [10–12] or to generate extensive amounts of underwater ice [13, 14]. Under such circumstances, colder temperatures along the upper section of the thermosyphon tube serve to promote a natural circulation within the tube, thus establishing an efficient heat withdrawal system. However, during the summer period the temperature field is inverted, thereby suppressing any natural convection and reducing the heat transfer efficiency to the much lower level of pure conduction.

The first exploratory theoretical study of the vertical closed tube thermosyphon was undertaken by Lighthill [3] who used his description of open-thermosyphon behaviour to postulate similar behaviour for the closed system. This suggestion was closely examined by Bayley and Lock [5] who proposed the model depicted in Fig. 1. In the lower section, heated fluid rises in an annulus adjacent to the tube wall while a replenishing core descends. In the upper section the flow is simply reversed, as indicated. It is therefore to be expected that the impeded and boundary layer flow regimes identified for the open system would also appear in the closed system, given that it may be described as a pair of coupled open elements.

At the junction of the upper and lower sections, the flow system is very complex but usually contains one or more of the following features: thermal instability creating a convective turnover which results in material from the ascending annulus entering the ascending core, while a corresponding transfer takes place downwards; mixing of the opposing annuli as they collide, particularly under turbulent conditions; and reflux of each annulus into its own core particularly for small temperature differences. These features have been examined by direct visualization [7], through heat transfer data [5, 7] and by means of internal temperature measurements [5, 6, 15]. The complexity and variability of the coupling mechanisms have seriously limited theoretical analysis of the closed tube thermosyphon [3, 8, 9, 16].

Almost all of the investigations of thermosyphon tubes have been restricted to situations in which the tube has lain parallel to a body force field, assumed to be constant. Under rotating conditions it is obvious that non-uniformity in the centrifugal field, together

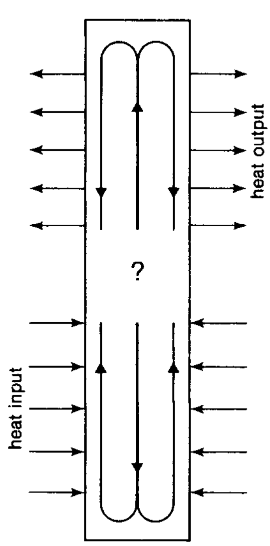

FIG. 1. Schematic flow model for vertical, closed tube thermosyphon.

NOMENCLATURE

d	tube diameter [m]
g	gravitational acceleration [m s^{-2}]
k	thermal conductivity [W m^{-1} K^{-1}]
L	tube length [m]
Nu	Nusselt number, $Q/\pi k(T_H - T_C)L_H$
Pr	Prandtl number, ν/κ
Q	heat flux [W]
Ra	Rayleigh number, $\beta g(T_H - T_C)d^3/\nu\kappa$
T	absolute temperature [K]
t	$(Ra)d/L$.

Greek symbols

β	thermal expansion coefficient [K^{-1}]
δ	layer thickness
θ	inclination to vertical
κ	thermal diffusivity [m^2 s^{-1}]
ν	momentum diffusivity [m^2 s^{-1}].

Subscripts

C	cooled
d	based on diameter
H	heated
m	mean.

with the effect of Coriolis forces, does not satisfy the assumption of a uniform force field. According to the conventional wisdom, a simulation of the Coriolis effect may be created by inclining a static tube to the vertical [7, 17, 18]. In a geotechnical context, it is a common requirement that thermosyphon tubes be inclined on berms or in the neighbourhood of foundations.

This paper is a systematic experimental investigation of the closed tube thermosyphon for inclinations ranging from the vertical to the horizontal. The study is restricted to low Rayleigh numbers. Its principal purpose is to use a representative liquid in a representative geometry to describe the effect of inclination on the Nusselt number–Rayleigh number relation. To assist with this description, a conceptual flow model is developed for laminar flow.

EXPERIMENTAL CONSIDERATIONS

The rig

The experiments were conducted in the FROST† Tunnel of the Department of Mechanical Engineering at the University of Alberta. This is a low temperature wind tunnel with a speed range of 10–60 m s^{-1} and a temperature range of -20 to 10°C. The thermosyphon tubes were installed in the octagonal wall panels of the tunnel as shown in Fig. 2. By means of a cylindrical hinge, the inclination of the tube could be set on any of a wide range of angles with respect to the normal to the tunnel wall. This arrangement provided a very convenient cooling system for the upper section of the tube which could thereby be studied at any inclination between the vertical and the horizontal.

The thermosyphons were made from a 2 cm i.d. copper tube cut into two equal lengths of 20 cm, thus fixing the length–diameter ratio at 10:1. The lower section was heated electrically using resistive metal tape separated from the tube wall by a layer of fibreglass tape. The heater tape was divided into two equal sections, each of which was connected in series with a variable resistance. This provided some flexibility in the control of power levels and temperature in the top and bottom sections of the heated tube, but did not create isothermal wall conditions; this point will be discussed later. Power to the heater tapes was supplied from the building mains converted into direct current by a Hewlett Packard 6268A d.c. unit. The power was measured using a voltmeter and an ohmmeter. No attempt was made to measure the heat leaving the upper tube. As noted earlier, this heat is removed by cold tunnel air and since the experiments were conducted under steady conditions it was only necessary to determine the net heat input.

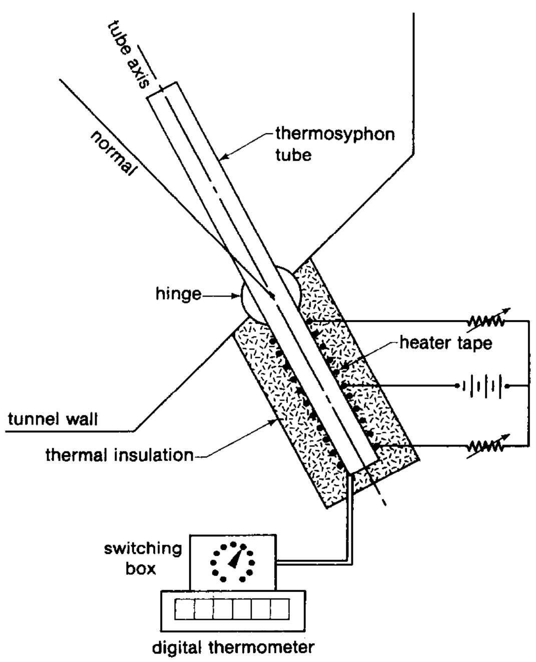

FIG. 2. Schematic of thermosyphon apparatus.

† An acronym for Fundamental Research on Solidification and Thawing.

Instrumentation and calibration

It is evident from Fig. 2 that the lower tube was wrapped with thermal insulation so as to reduce the heat leakage to the air, inside and outside of the tunnel. Prior to beginning the experiments proper, the heated tube was filled with granular insulation and calibrated by plotting the heat then supplied against the difference in temperature between the tube wall and the ambient air. Superimposed on this linear (conduction) plot are the incremental changes in power level produced by alterations in wind speed and temperature. This enabled the heat leakage under test conditions to be determined accurately and then subtracted from the gross power. Typically, the leakage power was of the order of 5% of the gross power.

Temperatures were measured throughout using copper–constantan thermocouples connected via a switching box to a Fluke 2175A digital thermometer. The thermocouples were located in the room air, the wind tunnel air, and on the outside of the thermosyphon tubes at 5 cm intervals in a plane containing the tube axis but perpendicular to the plane of tilt (on the stagnation lines for the cooled tube). These locations were chosen to provide the best estimates of average wall temperature, bearing in mind that the local wall temperature on the upper and lower surfaces of the tube would be expected to vary, respectively, above and below the mean (measured) value as the inclination varied. For both upper and lower tubes, the thermocouple wires were led out axially; on the lower tube they were installed prior to wrapping the tube with the fibreglass tape mentioned earlier.

Procedure and schedule

The experiments were conducted as follows. The tunnel was started up and the temperature set at a predetermined value; the wind speed was always fixed at 38 m s^{-1}. While the tunnel was approaching a steady state the electrical power to the heater tape was switched on and adjusted to some value in the anticipated range for the run (0–100 W). Periodic monitoring of the tube wall temperatures showed that at least 3 h were required for the entire system to approach close to steady conditions. When this period had elapsed the following readings were taken: tube wall temperatures, room air temperature, wind temperature, and gross power. The power was then altered and the measurement process repeated. For each data point, the local wall temperatures were used to calculate an average for the heated and cooled tube walls; these values were then used together with the wind and room air temperatures in estimating the heat leakage and hence the net power supplied. As noted earlier, isothermal walls were not attained, particularly in the region where the heated and cooled sections were joined. This fact, although limiting accuracy, does not compromise the data, as the results of previous work demonstrate [16].

The test series was conducted with water as the

Table 1. Test schedule

Test	Inclination (deg)†	t_d range ($\log_{10}$)	Mean temperature range, T_m (°C)
1	0	4.7–6.4	5.8–42.9
2	30	4.7–6.1	5.4–32.8
3	45	4.9–5.9	7.8–27.4
4	60	5.0–5.8	8.5–26.6
5	80	4.9–5.9	8.1–30.1
6	90	4.9–6.1	8.6–38.8

† From the vertical. $L_H/d = 10:1$. $L_H/L_C = 1:1$.

filling. The schedule is shown in Table 1 from which it is evident that the data cover a range of Ra_d or t_d extending over almost two orders of magnitude, and a full range of angles θ between the vertical and the horizontal: $t_d = (Ra)d/L_H$, where d is the tube diameter, L_H its heated length, and $Ra_d = \beta g(T_H - T_C)d^3/\nu\kappa$, in which β is the fluid coefficient of thermal expansion, g the gravitational acceleration, ν and κ the fluid momentum and thermal diffusivities, respectively, and T_H, T_C represent the heated and cooled wall temperatures, respectively.

FLOW DEVELOPMENT

Flow patterns in the inclined tube thermosyphon are nothing if not complex. Perhaps the easiest way to analyze them is by considering them divided into three distinct but interrelated regions: main flow, coupling, and end flow. In the vertical position, the main flow may often be treated as an axisymmetric counter-flow system, except in the mid-height region. This is illustrated in Fig. 1 which reveals that the main flow in the cooled upper section is simply the mirror image of the main flow in the heated lower section. The effect of inclination is to destroy the axisymmetry in both sections, anti-symmetrically [19–21]; the axis of the replenishing core in the lower section is displaced beneath the tube axis in the plane of the tilt, and a secondary flow is established in the form of a pair of vortices moving away from the closed end above the core. The reverse situation occurs in the upper section, so that the secondary motions across the coupling region are in opposite directions.

The complexity of flow in the coupling region is best treated in relation to the behaviour in the vertical position, where axisymmetry is preserved only outside of the coupling region. In principle, the mixing and refluence mechanisms mentioned earlier are not incompatible with axisymmetry but they do not demand it; moreover, the advective exchange process, which is not compatible with axisymmetry, is seldom an insignificant part of the overall thermal exchange process. In the open system [22], it has been observed that the emerging annular stream necks down into an axisymmetric jet shortly after leaving the mouth of the device. By way of compensation, the entering core material splits into several discrete streams which pierce the exiting material at several locations around the mouth thereby creating egg-shaped holes. The effect of placing a cooled tube over the mouth of a heated (open) thermosyphon tube would be to confine the emergent jet as a core, and to re-align the radial ingress of cold material more or less vertically from above. In other words, the egg-shaped holes would then lie in the junction plane of the two tubes, thus permitting a modified form of advective exchange between the two thermosyphon tubes.

The origin of this advective coupling in the closed thermosyphon appears to be associated with thermal instability in the vicinity of the junction plane [5]. The existence of a bundle of fluid filaments moving thus in opposite directions has been clearly demonstrated by Japikse *et al.* [7, 23] who observed that the number (or spacing) and stability of the bundle depends upon fluid properties, the Prandtl number in particular: lowering the Prandtl number tends to increase the number of filaments but decrease their stability, at least for non-metallic fluids. The existence of these filaments has been demonstrated numerically [9] for viscous liquids under laminar impeded conditions.

Continuity requirements demand that the total filament mass flux in one direction must equal that in the opposite direction. In many circumstances, this fact, coupled with periodicity around the tube circumference, leads to an even number of filaments distributed in alternating fashion around an annular region in the junction plane. Apparently, the effect of inclination is to re-organize the filament distribution [7]. Near the vertical position, the effect will simply be a small displacement of each filament essentially in the plane of the tilt: cold filaments move down, especially around the 'upper' surface of the tube perimeter; the reverse is true for hot filaments near the 'bottom' of the perimeter.

The lateral stability of the filaments is evidently not great, and is most likely constrained by the tube diameter, which limits their potential excursions. Thus, several small cold filaments moving away from the upper part of the perimeter may easily join together to form a larger cold filament and thereby provide space above for several hot filaments following a similar tendency. By the same token, hot and cold filaments near the vertical parts of the perimeter may alter their places and perhaps consolidate. With increasing inclination, the effect increases. A smaller number of larger filaments is gradually created, with the hotter filaments naturally tending towards the 'upper' part of the tube. Eventually, there are only two filaments, one moving in each direction. This situation appears to be well established long before the tube is horizontal: Japikse *et al.* [7] observed two filaments in water when $\theta = 6^\circ$.

Figure 3 is a schematic representation of advective exchange in the coupling region; for simplicity, only two filaments are shown. It indicates how the upward-flowing annulus may consolidate on one side (here drawn on the left) into a single filament which enters

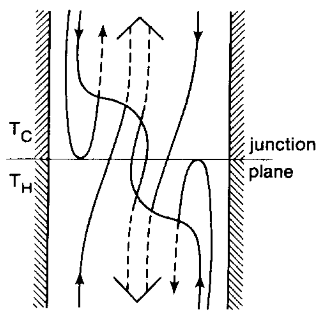

FIG. 3. Advective exchange in coupling region.

and becomes the core of the upper section, while the downward-flowing annulus consolidates on the other (right hand) side before flowing into the lower core. Given that the temperature of the lower section T_H is greater than the temperature of the upper section T_C, it is easy to see how the opposed annular layers would meet, begin to flow radially inwards, and then follow the dictates of thermal buoyancy; the hotter annulus is able to move inside the cooler annulus and vice versa. However, the process is not entirely advective, as the two refluent circulations indicate; and, of course, the creation of any local turbulence would be accompanied by mixing. The existence of this two-filament structure has also been observed numerically [20, 24] in a vertical thermosyphon under laminar impeded conditions.

Flow near the ends of the tubes may also depend upon the influence of $(T_H - T_C)$ by introducing a potential Rayleigh instability [3, 24, 25]. For low values of $(T_H - T_C)$, the axial temperature gradient at the end of a vertical tube may give rise to an axisymmetric ring vortex, as illustrated in Fig. 4(a). The effect of inclination is twofold; it destroys the axisymmetry and weakens the vortex. As indicated in Fig. 4(b), the inertia of the descending core ultimately, or perhaps initially, enables it to penetrate to the bottom where it creates a stagnation point, the location of which moves towards the lower corner as the inclination increases. Only a vestige, if anything, of the ring vortex then remains in the upper corner. Figure 4(b) illustrates the 'lowering' of the descending core (C) and the refluence (R) which occurs over the 'bottom' surface of the tube.

A composite flow for the entire thermosyphon may be obtained by combining the characteristics of the main flow, coupling and end flow. The resulting pattern is shown in Fig. 5 using two-filament coupling. This model, although speculative, is consistent with numerical predictions for other related systems [20, 21, 24] which have revealed that each filament contains a pair of vortices. The existence of this secondary vortical motion is crucial to the understanding of heat transfer performance, as discussed later.

Finally, it is worthwhile briefly discussing the alterations to this flow pattern which result from a transition to turbulence. A full treatment of the topic [23]

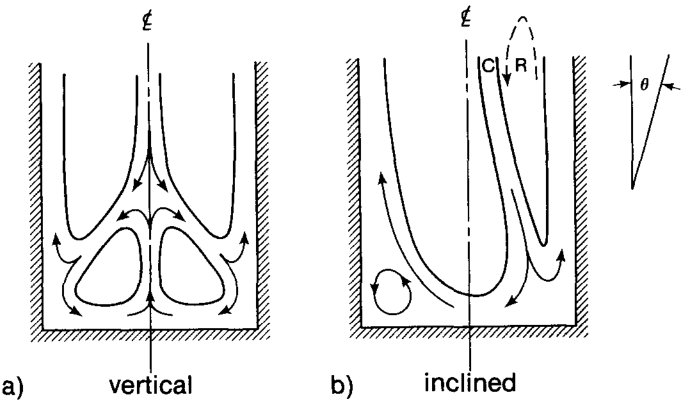

FIG. 4. End flows.

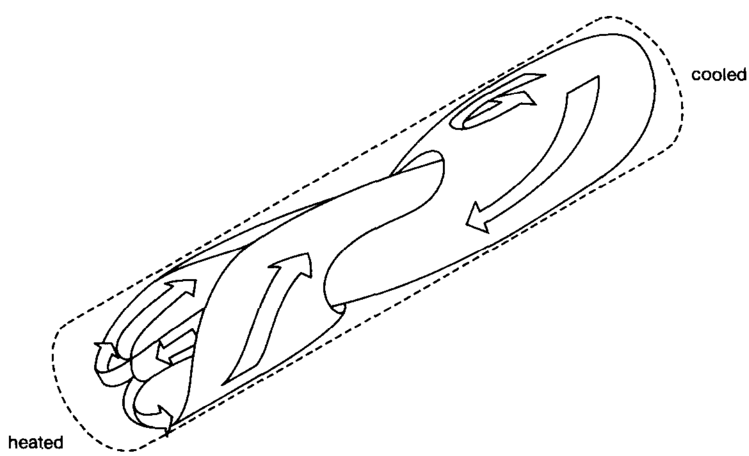

FIG. 5. Composite flow pattern.

is beyond this paper, and it is sufficient to note that transition in shorter vertical tubes is more likely to occur in the laminar boundary layer regime, e.g. $t_d \gg 10^5$, whereas in longer vertical tubes it may occur in the laminar impeded regime. A boundary layer transition would not alter the basic flow pattern suggested above; diffusive transport is simply replaced by a macroscopic, small scale, mechanism. On the other hand, transition in the impeded regime, where velocities are much lower, may lead to a large scale, low intensity type of turbulence which introduces randomness; not on a local scale, but on the scale of the tube diameter, thereby destroying rather than altering the flow pattern.

DISCUSSION OF RESULTS

Comparison with other work

Before considering the effect of inclination it is worth comparing various results obtained with a vertical tube. Using heat transfer data in the form Nu_d vs t_d, where $Nu_d = Q/\pi k(T_H - T_C)L_H$, Q is the total (net) heat transfer rate, and k the fluid thermal conductivity, these are shown in Fig. 6 from which it is immediately apparent that the present results are substantially lower than other experimental data. It is clear from the error bars, determined from a formal error analysis, that the difference cannot be explained by random experimental error. A careful re-examination of the experimental technique confirmed that

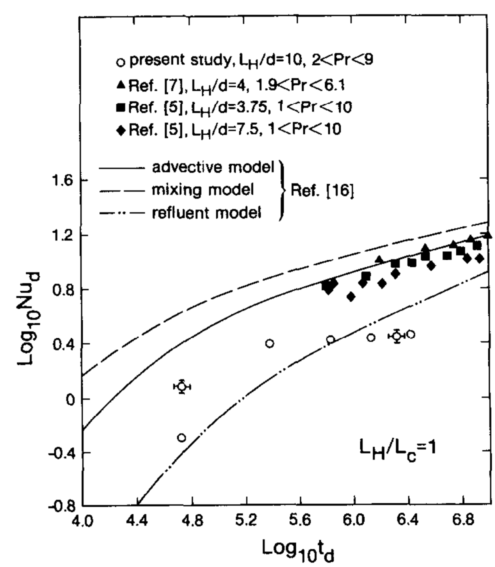

FIG. 6. Comparison with other work: vertical tube.

no systematic error had been made. It must therefore be concluded that the difference is the result of some systematic physical effect.

The four sets of experimental data shown in Fig. 6 were obtained over essentially the same temperature range, i.e. 0–100°C, and therefore $(T_H - T_C)$ is not significantly different among them. As indicated, they were all obtained with $L_H/L_C = 1.0$ and $3.75 < L_H/d < 10$. It would therefore appear that the geometrical differences were not too great although it must be noted that the tube diameters were different, the present experiments being conducted with narrower tubes. The difference between the ref. [5] data sets, is easily explained by the doubling of L_H/d but the difference between their data for $L_H/d = 7.5$ and the present data for $L_H/d = 10$ cannot be explained completely by the same trend.

Most of the data shown in Fig. 6 are in the range $10^5 \lesssim t_d \lesssim 10^7$ [5]. Under laminar boundary layer conditions, the thickness δ of the annulus is given by

$$\frac{\delta}{d} = \frac{1}{t_d^{1/4}}.$$

Using $t_d = 10^6$ as a representative value in the region of data overlap, it is evident that $\delta = O(d/30)$ and $Ra_d = O(10^7)$. No theoretical predictions or flow visualizations are currently available for these conditions. However, for $Ra_d \lesssim 10^5$ in shorter cavities the flow field may not be unique, or at least its marked tortuosity may be very sensitive either to the initial conditions of the experiment or to the boundary conditions. Thus, small temperature fluctuations, or the imposition of slightly different heating and cooling arrangements, particularly near the ends and junction region, may have been sufficient to create a different, but stable, flow under the same nominal conditions used elsewhere. Given the ambiguity in the equations governing a symmetric system heated from below [26], perhaps this behaviour is not surprising at lower Rayleigh numbers where refluence is likely to become increasingly important. This explanation is consistent with the numerical predictions [16] shown in Fig. 6 and suggests that the two-filament flow model of Fig. 5 may not always apply when the tube is vertical.

An alternative explanation may be found in the work of Martin [27] who concluded that the flow in a water-filled open thermosyphon underwent a transition to turbulence just below the point where the boundary layer regime meets the laminar impeded regime. If such a transition were to occur at this point in a closed system, it would have the effect of creating a turbulent impeded flow with characteristically lower and invariant Nusselt numbers. Thus, the existence of a scale of turbulence comparable with the smaller tube diameter used here may explain the departure from previously observed boundary layer behaviour seen in Fig. 6.

In addition, it should be mentioned that the water temperature spanned the inversion point (4°C) in some tests; the data thus affected are marked with a tag in Fig. 7 and a circle in Fig. 8. With the cold wall temperature in the range $0°C < T_C < 4°C$, it is to be expected that the circulation in the cold section would be partly reversed; in the extreme, as $T_C \to 0°C$, the global circulation may be upwards over the entire wall, heated and cooled, and downwards along the entire core [28]. This reversal in the upper section may account, in part, for the rapid decline in heat transfer rate at the lowest values of t_d measured. However, the heated wall temperature was never below 10°C even in these special cases, and hence the overall effect on circulation was not likely to be very great, as suggested by the fact that $\phi = (4 - T_C)/(T_H - T_C)$ was always less than 0.32 while $\phi \gtrsim 0.5$ is necessary for a significant inversion effect [29].

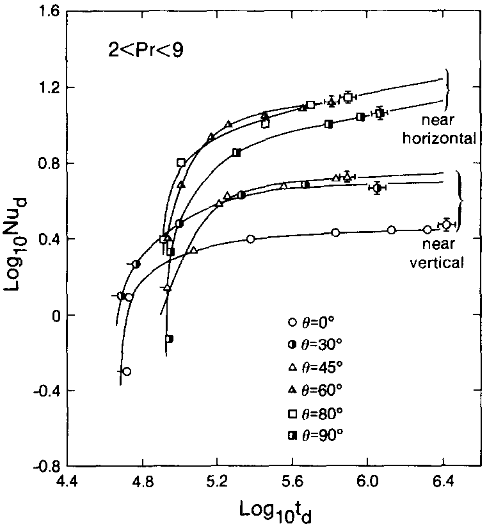

FIG. 7. Heat transfer characteristics of inclined tubes.

The effect of inclination

The heat transfer characteristics of inclined tubes are shown in Fig. 7 from which it is apparent that the data may be grouped in two categories: near vertical and near horizontal. The main effect of inclination is

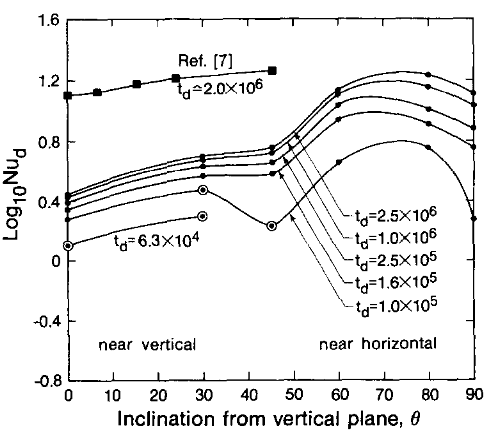

FIG. 8. Effect of inclination on heat transfer rate.

to raise the heat transfer rates above the value obtained for a vertical tube. This is seen more clearly by using the smooth curves drawn through the $Nu_d \sim t_d$ data to construct cross plots. The result is shown in Fig. 8 along with water data from Japikse *et al.* [7]. It is immediately obvious that the heat transfer efficiency initially increases with inclination from the vertical, a trend which appears to be counter-intuitive because the longitudinal component of the body force field driving the system decreases with increasing inclination. However, the effective body force field has two components, both of which are evidently important in amounts which vary with inclination.

Using the model developed above, it is to be expected that as the tube is inclined from the vertical the initial effect under laminar conditions would be complex but slight. The annular refluent zones would shrink slightly as the two-filament coupling mechanism evolved. These filaments would be subject increasingly to the organizing influence of a component of gravity acting normal to the tube axis; that is, secondary motion would appear. Opposing the gain attributable to a secondary motion is the decrease in longitudinal buoyancy. Overall, the increase in heat transfer rate is small, and slightly non-linear; this is consistent with previous observations [7] which were, however, believed to be for boundary layer conditions. It is suggested that a more plausible explanation follows from the assumption that the near vertical data were mostly in a turbulent impeded regime extending down to the lowest values of t_d where transition to a laminar impeded regime occurs. This assumption accounts for Nusselt numbers which are low and almost constant.

For inclinations greater than 45° the situation changes substantially as Fig. 8 reveals. The extent of the annular refluent zone would be further reduced, but it is believed that this is not the main cause of the rapidly increasing Nusselt number evident between 45° and 70°. Again referring to Fig. 5, it is evident that as the annular refluent zones shrink towards the tube ends, the length of the two opposed filaments increases. Normal to the tube axis, $g \sin \theta$ increases with inclination, giving rise to a vigorous secondary circulation in the form of a vortex pair in each filament [19–21]. This evertive augmentation is evidently the cause of the significant rise in heat transfer for θ between 45° and 70°.

It is also evident that this secondary motion will continue to increase in strength as the inclination increases further. However, the longitudinal component of gravity $g \cos \theta$ continues to decrease as the horizontal position is approached. The primary flow is thus driven by a weakening field which is eventually replaced by the much smaller indirect buoyancy effect dependent upon the horizontal temperature gradient. The opposition of a strengthening secondary flow and a weakening primary flow results in the maximum displayed in Fig. 8. Beyond the maximum, it is diminishing the strength of the primary circulation which causes the decrease in heat transfer rate.

When the tube is horizontal, annular refluence ceases to exist and the system consists simply of a horizontally-driven, two-filament primary loop superimposed on which is a vertically-driven secondary flow consisting of two pairs of longitudinal vortices with opposite signs, and one above the other [19–21]. Under these conditions, the cold core shown in Fig. 4(b) runs along the bottom of the tube and Fig. 5 is modified accordingly; no stagnation point then exists on the end faces. The $Nu_d \sim t_d$ data at, or near, the horizontal position reveal a positive slope which, in the upper reaches, e.g. $t_d > 10^{5.4}$, is approximately equal to 0.2, the value normally associated with laminar boundary layer natural convection over horizontal surfaces.

Finally, it is worth recalling the alterations in the location of the lower t_d 'transition' noted earlier. This evidently represents a change to laminar impeded flow [3, 5, 21]. Figure 7 indicates that the near-vertical transitional point is quite separate from the point associated with large inclinations, the latter being virtually independent of angle. It is suggested that the near-vertical ($\theta < 30°$) transition is essentially controlled by the near-vertical (and probably turbulent) flow field in the annulus and core. For positions nearer the horizontal, and especially for $\theta \geqslant 45°$, the two-filament model of Fig. 5 suggests a marked change in the flow fields. Apparently, the primary circulation does not change significantly over a wide range of inclinations near the horizontal [20, 21]; this therefore corresponds to a transitional shift from the near-vertical value to a new value valid for large inclinations and determined from the near-horizontal flow field. The transition was always steeper than expected because the lowest points were taken with the cooled section wall temperature below the inversion temperature but this did not appear to alter the distinction between the low and high θ transitions.

CONCLUSIONS

The experimental data presented fall in the low Rayleigh number range where slowly varying Nusselt number behaviour was found to end abruptly at the low end. It is suggested that this transition marks the upper limit of a laminar impeded regime which is different in near-vertical and near-horizontal tubes, the difference reflecting the marked alteration in the primary flow field.

To explain the complex behaviour of the system a flow model has been developed from related numerical studies in the laminar impeded regime. Essentially, this is based on the reconciliation of three flows: the main flow in each tube, the end region flow, and the flow pattern which couples the heated section to the cooled section. The axisymmetric main flow which occurs in a vertical tube is thus modified to account for secondary motion and core displacement at both ends. In the coupling region, the model accommodates the effect of thermal buoyancy as the source of a pattern of interlaced streams, or filaments, which cross through each other. In this way it is possible to account for the influence of both the advective and refluence mechanisms, the balance between determines the overall efficiency of the system.

Near the vertical position, the flow system may be more complex than the two-filament flow model indicated in Fig. 5. One suggestion is that multi-filament coupling may then exist; the flow pattern may not be unique, thus leading to the possibility of branching in the heat transfer rate. Alternatively, a turbulent impeded regime may have been entered. In any event, the results suggest the gradual emergence of a more efficient two-filament flow which accompanies increasing inclination and more than offsets the effect of a decrease in the longitudinal component of the gravitational field.

For greater inclinations, the flow model was found to be very helpful in interpreting the heat transfer data. In particular, it suggests that further increases in the heat transfer rate are attributable to the increasing evertive augmentation associated with secondary circulation in each of the two filaments. It also provides an explanation of the maximum. Beyond this point, the continued increase in secondary motion is more than offset by the decrease in the primary circulation which is eventually driven solely by the weak effect of horizontal temperature gradients; the heat transfer rate then decreases.

Acknowledgements—This work was carried out under the auspices of the Natural Science and Engineering Research Council of Canada to whom we are indebted. We also wish to thank Mr T. Nord, Mr A. Muir and the workshop staff of the Department of Mechanical Engineering. Special thanks are due to Ms Y. Liu who assisted with the acquisition and presentation of the data.

REFERENCES

1. E. Schmidt, Heat transmission by natural convection at high centrifugal acceleration in water-cooled gas turbine blades, *Proc. Instn Mech. Engrs* **IV,** 361–363 (1951).
2. H. Cohen and F. J. Bayley, Heat transfer problems of liquid cooled gas turbine blades, *Proc. Instn Mech. Engrs* **169**(20), 1063–1080 (1955).
3. M. J. Lighthill, Theoretical considerations on free convection in tubes, *Q. J. Mech. Appl. Math.* **6**(4), 398–439 (1953).
4. B. W. Martin, Free convection in an open thermosyphon tube with special reference to turbulent flow, *Proc. R. Soc.* **A230,** 502–530 (1955).
5. F. J. Bayley and G. S. H. Lock, Heat transfer characteristics of the closed thermosyphon, *J. Heat Transfer* **87,** 30–40 (1965).
6. D. Japikse and E. R. F. Winter, Single-phase transport processes in the open thermosyphon, *Int. J. Heat Mass Transfer* **14,** 427–441 (1971).
7. D. Japikse, P. A. Jallouk and E. R. F. Winter, Single-phase transport processes in the closed thermosyphon, *Int. J. Heat Mass Transfer* **14**(7), 869–887 (1971).
8. A. D. Gosman, F. C. Lockwood and D. G. Tatchell, A numerical study of the heat transfer performance of the open thermosyphon, *Int. J. Heat Mass Transfer* **14**(10), 1717–1721 (1971).
9. G. D. Mallinson, A. D. Graham and G. de Vahl Davis, Three-dimensional flow in a closed thermosyphon, *J. Fluid Mech.* **109,** 259–275 (1981).
10. G. F. Biyanov, Liquid cooling unit for freezing thawed ground and cooking plastically frozen ground for construction in areas with harsh climates, *Proc. Second Int. Permafrost Conf.*, National Academy of Science, p. 641 (1973).
11. H. O. Jahns, T. W. Miller, L. D. Power, W. P. Rickey, T. P. Taylor and J. A. Wheeler, Permafrost protection for pipelines, *Proc. Second Int. Permafrost Conf.*, National Academy of Science, pp. 673–684 (1973).
12. R. L. Reid, J. S. Tennant and K. W. Childs, The modeling of a thermosyphon type permafrost protection device, *J. Heat Transfer* **97,** 382–385 (1975).
13. G. S. H. Lock, The BIVA project, *Proc. IAHR Ice Symp.*, Vol. II, pp. 269–280 (1986).
14. G. S. H. Lock, Control of spring run-off in northern rivers: the ice veil concept, *Polar Record* 451–457 (1986).
15. G. S. H. Lock and G. A. S. Simpson, Performance of a closed tube thermosyphon with large length–diameter ratios, *J. Offshore Mech. Arctic Engng* **111,** 22–28 (1989).
16. G. A. S. Simpson, Geometrical effects in the closed tube thermosyphon, M.Sc. Thesis, University of Alberta, Edmonton, Alberta (1986).
17. J. F. Alcock, General discussion on heat transfer, *Proc. Instn Mech. Engrs* **IV,** 378 (1951).
18. B. W. Martin and D. J. Cresswell, Influence of Coriolis forces on heat transfer in the open thermosyphon, *The Engineer* **204,** 926–930 (1957).
19. P. Bontoux, C. Smutek, B. Roux and J. M. Lacroix, Three dimensional, buoyancy-driven flows in cylindrical cavities with differentially-heated end walls—I. Horizontal cylinders, *J. Fluid Mech.* **169,** 211–227 (1986).
20. P. Bontoux, C. Smutek, A. Randiamampianina, B. Roux, G. P. Extremet, A. C. Hurford, F. Rosenberger and G. de Vahl Davis, Numerical solutions and experimental results for three-dimensional buoyancy-driven flows in tilted cylinders, *Adv. Space Res.* **6**(5), 155–160 (1986).
21. G. S. H. Lock and J.-C. Han, Buoyant flow of air in a long, square-section cavity aligned with the ambient temperature gradient, *J. Fluid Mech.* **207,** 489–504 (1989).
22. B. W. Martin and F. C. Lockwood, Entry effects in the open thermosyphon, *J. Fluid Mech.* **19**(2), 246–256 (1963).
23. D. Japikse, Heat transfer in open and closed thermosyphons, Ph.D. Thesis, Purdue University, Lafayette, Indiana (1968).
24. G. S. H. Lock and Litong Zhao, The laminar flow field in a near-vertical, closed tube thermosyphon, *Proc. 7th Int. Conf. on Math. and Comput. Modelling*, Chicago, Vol. 14, pp. 822–825 (1990).
25. G. Muller, G. Neumann and W. Weber, Natural convection in vertical Bridgman configurations, *J. Cryst. Growth* **70,** 78–93 (1984).
26. G. S. H. Lock and J.-C. Han, The effects of tilt, skew and roll on natural convection in a slender, laterally-heated cavity, *Math. Comput. Modelling* **13**(2), 23–32 (1990).
27. B. W. Martin, Free convection in an open thermosyphon with special reference to turbulent flow, *Proc. R. Soc.* **A230,** 502–530 (1955).
28. G. S. H. Lock and Y. Liu, The effect of geometry on the performance of the closed tube thermosyphon at low Rayleigh numbers, *Int. J. Heat Mass Transfer* **32**(6), 1175–1182 (1989).
29. C. R. Vanier and C. Tien, Effect of maximum density and melting on natural convection heat transfer from a vertical plate, *Chem. Engng Prog. Symp. Ser. 82* **64,** 240–254 (1968).

QUELQUES CARACTERISTIQUES D'UN THERMOSIPHON INCLINE, FERME, DANS DES CONDITIONS DE FAIBLE NOMBRE DE RAYLEIGH

Résumé—On décrit une analyse expérimentale du transfert de chaleur en monophasique dans un thermosiphon tubulaire fermé, incliné avec plusieurs angles par rapport à la verticale. Avec de l'eau comme fluide de remplissage, le système est étudié pour un domaine de faibles nombres de RAYLEIGH, s'étendant sur deux ordres de grandeur. On présente les données de transfert thermique pour un tube ayant des longueurs égales de chauffage et de refroidissement et on discute à l'aide d'un modèle de l'écoulement interne.

UNTERSUCHUNGEN AN EINEM GENEIGTEN GESCHLOSSENEN THERMOSYPHON BEI KLEINEN RAYLEIGH-ZAHLEN

Zusammenfassung—Es wird über eine experimentelle Untersuchung des einphasigen Wärmetransports in einem geschlossenen Thermosyphon berichtet, der unter verschiedenen Winkeln gegenüber der Senkrechten geneigt ist. Als Arbeitsstoff wird Wasser verwendet. Das System wird in einem Bereich kleiner Rayleigh-Zahlen untersucht, der sich über fast zwei Größenordnungen erstreckt. Es werden Ergebnisse für den Wärmeübergang in einem Rohr vorgestellt, bei dem Heiz- und Kühlzone gleich lang sind. Diese Ergebnisse werden auf der Grundlage einer Modellvorstellung über die interne Strömung diskutiert.

НЕКОТОРЫЕ ХАРАКТЕРИСТИКИ НАКЛОННОГО ЗАМКНУТОГО ТРУБЧАТОГО ТЕРМОСИФОНА ПРИ НИЗКИХ ЧИСЛАХ РЭЛЕЯ

Аннотация—Экспериментально исследуется однофазный теплоперенос в замкнутом трубчатом термосифоне при различных углах наклона относительно вертикали. В качестве рабочей жидкости используется вода. Исследование проводится в диапазоне малых значений числа Рэлея, включающем почти два порядка величины. Даются данные по теплопереносу в трубе с участками нагрева и охлаждения одинаковой длины, и обсуждается концептуальная модель внутреннего течения.